SAND99-0807C

Fire-induced Response in Foam Encapsulants

T. Y. Chu, M. L. Hobbs, K .L. Erickson, T. A. Ulibarri, A. M. Renlund
W. Gill, L. L. Humphries, and T. T. Borek
Sandia National Laboratories, Albuquerque, NM 87185

ABSTRACT

The paper provides a concise overview of a coordinated experimental/theoretical/numerical program at Sandia National Laboratories to develop an experimentally validated model of fire-induced response of foam-filled engineered systems for nuclear and transportation safety applications. Integral experiments are performed to investigate the thermal response of polyurethane foam-filled systems exposed to fire-like heat fluxes. A suite of laboratory experiments is performed to characterize the decomposition chemistry of polyurethane. Mass loss and energy associated with foam decomposition and chemical structures of the virgin and decomposed foam are determined. Decomposition chemistry is modeled as the degradation of macromolecular structures by bond breaking followed by vaporization of small fragments of the macromolecule with high vapor pressures. The chemical decomposition model is validated against the laboratory data. Data from integral experiments is used to assess and validate a FEM foam thermal response model with the chemistry model developed from the decomposition experiments. Good agreement was achieved both in the progression of the decomposition front and the in-depth thermal response.

KEY WORDS: Polyurethane Foam, Decomposition Chemistry, Thermal Response

1. INTRODUCTION

In most foam-filled engineered systems, components encapsulated in foam are confined typically in an external metal enclosure (skin). The purpose of the Sandia foam material response program is to develop a high fidelity computational tool for fire-induced response of foam filled engineering systems. Fire-induced response of the system will include the combined thermal and mechanical response of the foam, components, and the enclosure. A complete system response model will involve coupled chemical, thermal, and mechanical submodels. Direct mechanical interaction between the foam and the enclosure is probably not important because gas pressure will be the main driving force for enclosure deformation and failure. However, pressure-induced deformation of the foam can be important.

A coordinated experimental/theoretical/numerical program at several levels (scales) is used to address the problem:

- Laboratory decomposition chemistry experiments:
  These are essentially spatially isothermal experiments to investigate the foam decomposition mechanism and kinetics. Mass loss and energy associated with foam decomposition and chemical structures of the virgin and decomposed foam are determined.
- Decomposition chemistry submodel:
  Decomposition chemistry is modeled as the degradation of macromolecular structures by bond breaking followed by vaporization of small fragments of the macromolecule with high vapor pressures. The chemical structure of the polymer is determined from synthesis details. The chemical decomposition model is validated against the laboratory decomposition chemistry data.
- Integral experiments:
  Experiments with well-characterized boundary conditions and relatively simple geometry are performed to generate data on the thermal response of polyurethane foams exposed to fire-like heat fluxes on a scale consistent with applications. Initially the integral experiments are used to gain physical insights to the problem to establish the overall requirements of the computational model. Once a model is established, well-instrumented and carefully performed integral experiments are used to validate the computational model.

This paper reports the first step in developing the simulation tool for fire-induced response of foam-filled engineered systems. The main emphasis is on thermal response of the foam and a single encapsulated component with only preliminary consideration of enclosure pressurization effects. Integral experiments with a simple 1-D heating of a foam assembly are presented. Laboratory decomposition experiments are then discussed, and it is shown how the results can be understood through considering a detailed molecular-level decomposition chemistry model. The detailed model is then incorporated in a finite element heat conduction code and used to predict the results of the integral experiment.

2. INTEGRAL-SCALE EXPERIMENTS

Two types of experiments were performed: (1) one-dimensional thermal transport experiments where the end of a foam cylinder was exposed to a high heat flux to examine the in-depth thermal response of the foam and (2) component response experiments where a foam cylinder, with an encapsulated cylindrical component, is heated at one end and the thermal response of the foam and the embedded cylinder were measured. Real time X-ray was used to track the progression of the decomposition front and to examine the density profile in the decomposition zone in both experiments. The majority of the experiments were vented to the ambient, although some preliminary confined and pressurized experiments have been performed. Gas bombs and desorption tubes were used to collect decomposition product samples; posttest residuals were also examined. A high density, 353 kg/m^3 (22 lb/ft^3) closed cell polyurethane foam was used in most experiments; an 11 lb/ft^3 foam has been used in some experiments. This section will present the design of the experiments and the physical interpretation of the thermal transport processes.

Experimental Design

Ambient Pressure Vented 1-D Thermal Transport Experiment

A schematic of the experimental assembly is shown in Figure 1. The foam sample is a machined 8.76-cm diameter, 14.61-cm high cylinder. The foam cylinder is contained in a sample cup. The cup consists of a 6-mm thick steel or stainless steel bottom, which is force fitted into a 7.3-cm long, thin wall (0.5 mm) stainless steel tube. Up to six 6-mm holes are drilled through the side of the stainless steel tube, near the cup bottom, to vent decomposition gases. The number and size of the vents were chosen to ensure the pressure within the cup is near ambient. The cup bottom is heated by an array of radiant heat lamps. Outside and inside surfaces of the cup are painted with Pyromark^{R} black paint to give a consistent emissivity for all the radiating surfaces. The relatively thick bottom promotes uniform heating of the foam sample. The uninsulated thin stainless steel sidewall limits lateral conduction. Experiments were performed with the heated surface facing downward (as shown in Figure 1), upward, or parallel to gravity (facing sideward).

Thermocouples installed in radial holes drilled from the side of the cylinder, nominally 6.4 mm apart, are deployed along the central axis of the foam sample and nominally 12.7 mm apart along a line 2.5 cm off the central axis (to check for radial temperature variations). The cup bottom is instrumented with two thermocouples installed parallel to the cup bottom one-third and two-thirds through the thickness of the bottom. Six thermocouples held against the side of the cup by welded stainless straps measure lateral temperature distribution in the sidewall to provide the boundary conditions for modeling the experiment. All the thermocouples are 0.5 mm OD, Type K sheathed thermocouples with grounded junctions. Because of the difficulties in drilling a 0.5-mm hole with precision, the exact locations of the thermocouples are determined from pretest x-ray images. A heat flux gauge located next to the steel cup is used to monitor and control the incident heat flux to the vessel bottom. The actual incident heat flux on the cup bottom is deduced from a pretest comparison calibration between a gauge installed through a hole in the bottom of a surrogate steel cup and the heat flux gauge located next to the steel cup.

Component Response Experiments

An instrumented, 304 stainless steel slug is embedded coaxially, 3 cm below the top surface of a foam cylinder. Thermocouples are installed radially, with tips located midway through the annular foam between the embedded cylinder and the OD of the foam cylinder, nominally 12.7 mm apart laterally. Figure 2 shows an X-ray image of a component response experiment.

Confined and Pressurized Experiment

A schematic of the experiment is shown in Figure 3. The wall of the sample cup extends beyond the nonheated end of the foam cylinder, and epoxy resin is used to form a sealed end cap for the experimental assembly. The vent holes are replaced by four 3 mm ID stainless vent tubes. The tubes are connected to a water-cooled (~ 5°C) tube condenser. Before the experiment the condenser is charged with nitrogen to a desired test pressure. During the experiment, pressure is maintained by venting the gas reaction product through a pressure control valve.

Experimental Results

Ambient Pressure Vented 1-D Thermal Transport Experiments

Experiments exposed the closed cell, 353-kg/m^3 (22-lb/ft^3) foam to incident heat fluxes ranging from 5 w/cm^2 to 25 w/cm^2. A typical set of in-depth thermal response curves (Test 5, heated surface facing down) is plotted in Figure 4. Except for early times the thermal histories at different locations are essentially identical and displaced in time only. The behavior is suggestive of an ablation process, and the temperature history at an in-depth point was determined by Landau (1950) to be

$$T(t) = T_0 + (T_m - T_0) \cdot e^{\frac{-v \cdot [y - v \cdot (t - t_0)]}{\alpha}},$$

where T_0 is the far field (constant) temperature, T_m an apparent ablation temperature (200° C for the present work), y is in-depth location, v is the front velocity, α is the foam thermal diffusivity, t is time, and t_0 is a virtual initiation time to account for the starting transient. The coordinate transformation, $[y-v \cdot (t-t_0)]$, simply states that under steady-state ablation, the temperature distribution in the material is invariant with respect to the moving front. The agreement between the Landau model and the observed temperatures is quite good, see Figure 4. The velocity of the decomposition front is determined from the x-ray images and/or the arrival time of specific isotherms (temperatures) at specific (thermocouple) locations. The recession velocity was found to vary essentially linearly with the incident heat flux. As shown in Figure 5 for the same incident heat flux, the recession velocity is essentially constant and nearly independent of heating surface orientation. Although when the surface is parallel to gravity, the recession velocity is higher near the top suggesting the possibility of a viscous decomposing liquid layer of increasing thickness flowing down the decomposing surface but this hypothesis has yet to be examined in detail.

The 1-D thermal transport experiments suggest that the computational model must have the capability to track a moving decomposition front. The Landau correlation provides a measure of the thickness of the decomposition front, therefore, a measure of the mesh size. As the foam recesses the enclosure through which the heated surface radiates against the decomposing foam increases in size. Therefore, the computational model must be able to perform dynamic enclosure radiation calculations.

Component Response Experiments

Because the decomposition zone is very thin for the relatively high incident heat flux experiments reported here, the presence of the embedded component does not manifest itself until the component is nearly exposed. Once the component is exposed, the decomposition front is no longer planar. The progression of the decomposition front is retarded in the region adjacent to the component owing to the thermal capacitance of the component and radiation blocking. Details of the foam and component thermal responses are discussed in **Section 4,** where comparisons are made between model predictions and experiment.

Confined and Pressurized Experiments

Preliminary confined experiments were performed for pressures from ambient to about three atmospheres, using nominally 11-lb/ft^3 (176-g/cm^3) foam. The experiments are characterized by a densified decomposition zone whose thickness increases with time, see Figure 6. The progression of the decomposition zone was found to be decreasing with time. In fact, the front location is well correlated by $(t-t_0)^{1/2}$, typical of a phase change behavior, see Figure 6. When the pressure increases beyond two atmospheres, X-ray indicates the possibility of infiltration of dense material into unreacted foam as a result of cell wall breakage. Future experiments are planned to further explore confinement and pressurization effects.

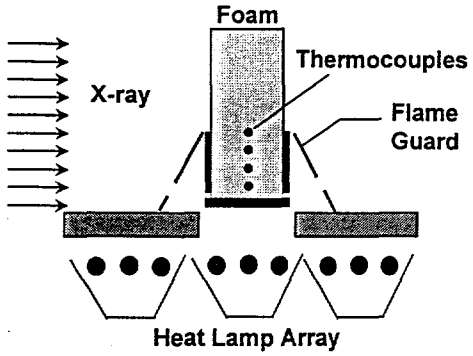

Figure 1 Schematic of ambient pressure vented experiments.

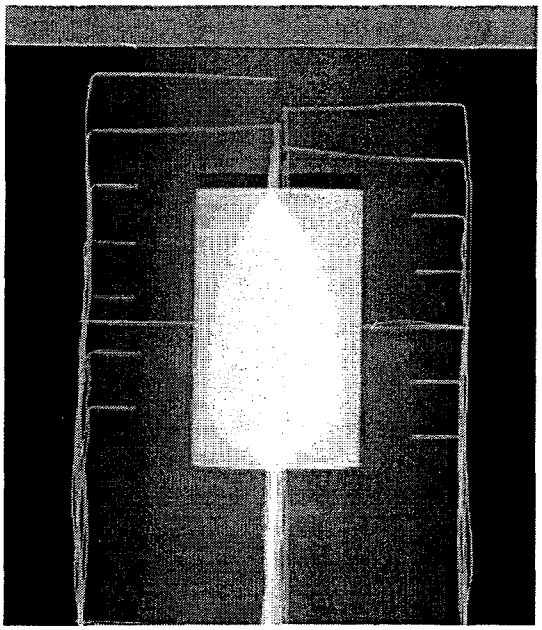

Figure 2 X-ray of a component response experiment.

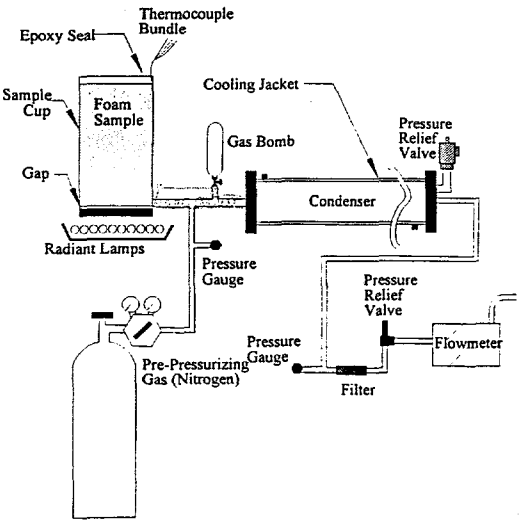

Figure 3 Schematic of the confined and pressurized experiment.

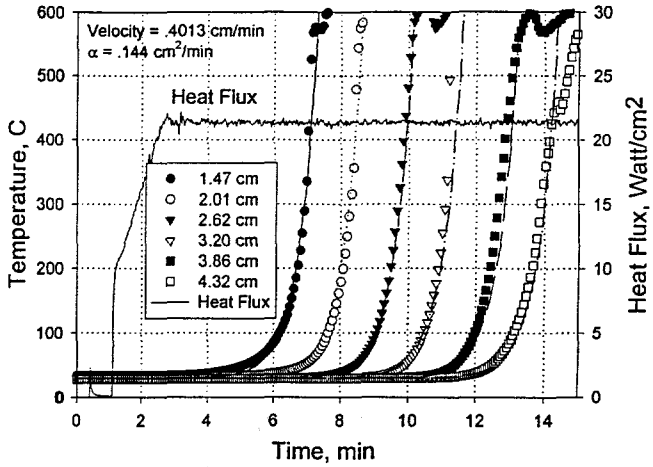

Figure 4 Comparison of experimental results with Landau ablation model for test 5.

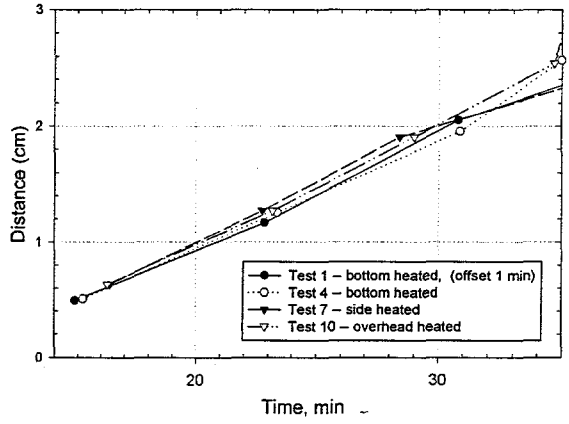

Figure 5 Comparison of decomposition front progression for different orientations.

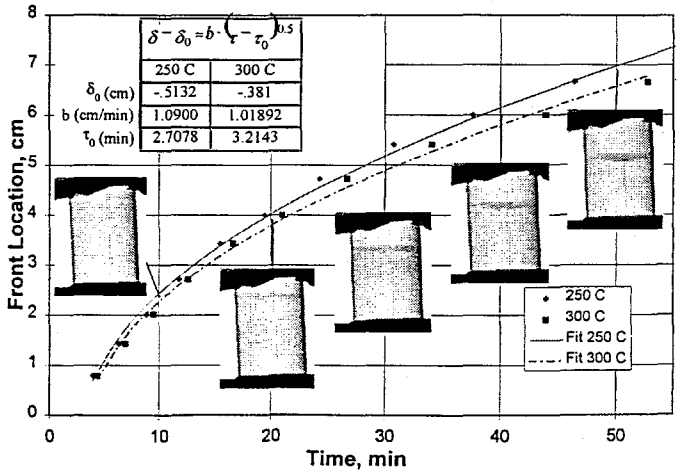

Figure 6 Progression of decomposition front (as observed from 250o C and 350° C isotherm) under confinement and pressurization (67 kPa).

3. DECOMPOSITION CHEMISTRY EXPERIMENTS

Numerical simulations require foam decomposition chemistry submodels that must be developed from experimental investigation of foam decomposition mechanism and kinetics. Because no single experimental technique can provide all of the required data, a variety of techniques and diagnostics were selected to obtain data for developing a foam submodel that is consistent with the detail needed for the numerical simulations. The foam decomposition experiments were designed to: (1) determine the major chemical reaction mechanisms and kinetics, particularly species evolution and molecular weight distributions, controlling polymer decomposition; (2) determine the enthalpy changes associated with decomposition; and (3) examine the effects of the coupling of chemical reactions, vapor-liquid-solid equilibria, and mass transfer.

Experimental Techniques and Diagnostics

The experimental techniques and diagnostics were selected to provide a variety of experimental conditions and reaction regimes. Experiments were done with samples of foam having a density of either 176 (low) and 353 (high) kg/m^3. (1) Thermal gravimetric analysis (TGA) experiments involving small (5-20 mg) samples have been done in unconfined and partially confined sample configurations. The unconfined configuration involved samples in open platinum pans and was used to examine initial decomposition mechanisms under conditions that minimize effects of mass transfer and reversible and secondary reactions. The partially confined configuration involved crimp-sealed aluminum pans having lids with circular orifices as small as 0.06 mm and was used to examine the effects of any reversible or secondary reactions that would result from limiting mass transfer of the decomposition products. Real time analysis of the evolved gases was done using Fourier Transform Infrared (FTIR) spectroscopy. Periodic sampling and analysis of evolved gases were done using desoprtion tubes followed by gas chromatography-mass spectrometry (GC-MS). Solid residues were examined postmortem using infrared microprobe (IRMP). (2) Differential thermal analysis (DTA) experiments were used to determine the enthalpy changes occurring under conditions similar to those in the TGA experiments. (3) High-pressure cell, constant-load, piston-displacement experiments involving larger samples (50-100 mg) were used to examine decomposition under highly confined conditions in which mass transfer is highly limited, and the effects of any reversible or secondary reactions would be most significant. (4) Tube furnace experiments were done with relatively large samples (1 to 3 g) to obtain data for reaction products and molecular weight distributions under intermediate conditions in which the size of the foam sample was large enough to limit mass transfer to the surrounding atmosphere. Cold traps were used to collect organic products for subsequent analysis using GC/MS and gel permeation chromatography (GPC), which was feasible because of the larger sample size. Real time analysis of noncondensable gases was done using FTIR spectroscopy, and periodic sampling and analysis of evolved gases were done using desorption tubes followed by GC-MS. Solid residues were examined postmortem using IRMP.

Experimental Results and Decomposition Mechanisms

The results obtained using each of the above experimental techniques and diagnostics are summarized below, and the decomposition mechanisms inferred from those results are discussed.

TGA Experiments

The TGA experiments were done using a variety of heating conditions that included: (1) constant heating rate (5, 20, or 50 °C/min from ambient to 600° C or higher); (2) "one-step isothermal" (constant heating rate of 20 to 50 °C/min to a temperature between 270 and 330° C, followed by a constant temperature period of one hour or more); and (3) "two-step isothermal" (constant heating rate of 20 to 50 °C/min to a temperature of 300° C, followed by a constant temperature period of one hour or more, constant heating rate of 20 to 50 °C/min to a higher

temperature between 380 and 420° C, followed by a second constant temperature period of one hour or more).

Results from TGA experiments using unconfined samples subjected to constant heating rates are illustrated in Figure 7a, which shows the rate of mass loss versus temperature for a sample heated at 20° C/min. The "double-peaked" curve indicates that at least two decomposition steps probably occur. This is further supported by the FTIR spectra shown in Fig. 8, which were collected during the experiment. The spectrum shown in Figure 8a is typical of the spectra obtained during sample heating in the range of 250 to 350° C and is dominated by the toluene diisocyanate (TDI) signal at about 2280 cm^{-1}. The spectrum shown in Figure 8b is typical of the spectra obtained during sample heating above 350° C and shows a CO_2 signal (about 2360 cm^{-1}) and a strong carbonyl signal at about 1750 cm^{-1}. The signal at 3000 cm^{-1} is due to C-H stretching. Independent TGA experiments were done using desorption tubes to sample evolved gases. Subsequent GC-MS confirmed that in the temperature range of 250 to 350 ° C, toluene diisocyanate was the major decomposition product, which indicated loss of the urethane linkage due to the urethane retrograde reaction. At temperatures above 350° C, major products included cyclopentanone and trimethoxypropane, which are consistent with scission of the ester linkages in the polymer.

Results from TGA experiments using partially confined samples subjected to constant heating rates are illustrated in Figure 7b, which shows the rate of mass loss versus temperature for a sample that was sealed in aluminum pans with a 0.35-mm orifice and heated at 20° C/min. The rate of mass loss as a function of temperature for the partially confined sample is significantly different than for the unconfined sample in Figure 7a. This could, in part, be due to slower vaporization of volatile decomposition products. However, the FTIR spectra collected during the experiment indicate a substantial change in the products evolving at lower temperatures. The spectrum in Figure 9a is typical of the spectra obtained between 250 and 350° C and shows a substantial CO_2 signal in addition to the TDI signal. The spectrum in Figure 9b is typical of those obtained at temperatures above 350° C. The general trend observed in the partially confined experiments was that the signal for CO_2 increased with confinement, and the signal for TDI decreased. The amount of carbonaceous residue also increased with confinement. These results could be due to: (1) secondary reactions following the urethane retrograde reaction or (2) since the urethane retrograde reaction is reversible, a parallel decomposition path producing CO_2 and a condensed-phase amine product.

DTA Results

Limited DTA experiments were done under conditions similar to the TGA experiments. Comparison of results from similarly done TGA and DTA experiments indicated an overall endothermic energy of reaction of about 100 cal/g.

High-Pressure, Constant Load Cell Results

The constant load cell experiments generally involved constant heating at about 6 to 8 °C/min to temperatures in the range of 270 to 310° C. The applied pressures varied from about 1.4 to 14 MPa. Significant piston displacement occurred at these pressures and could have been due to low molecular weight gases, such as CO_2, which can exert sufficiently high pressures. These results are consistent with and extend the results from the partially confined TGA experiments.

Tube Furnace Results

The tube furnace experiments generally involved the following steps: (1) heating the sample at 5 °C/min to 300° C, (2) maintaining a constant temperature of 300° for several hours, (3) cooling

to room temperature (for weighing and sampling for IRMP analysis), (4) reheating the remaining sample at 5 °C/min to 600° C, (5) maintaining a constant temperature of 600° for several hours, and (6) cooling to room temperature (for weighing and sampling for IRMP analysis). Gases that evolved from the tube furnace passed through two traps that were cooled with dry ice and acetone. Noncondensable gases were monitored with FTIR.

During heating to 300° C, mass balances showed that about 25 percent of the sample evolved as noncondensables (which FTIR spectra indicated were primarily CO_2), about 50 percent condensables, and 25 percent remained in the furnace as condensed-phase residue. IRMP analyses showed that the condensables primarily contained isocyanate and carbonyl species as well as amine and alcohol containing species. Periodic sampling with desorption tubes and subsequent GC-MS indicated that the primary condensable products changed with time. The time sequence in which those products evolved was as follows: (1) TDI; (2) 3-methyl-2-butenal and cyclopentanone; (3) 1,4-dioxane and trimethoxypropane. GPC indicated that molecular weight of condensables for both high and low density foam are relatively low (MW < 800, relative to polystyrene) with very narrow MW ranges (polydispersity < 1.3). Also, MS and GC-MS of the condensables indicated constituents similar to those identified in products from component-scale tests. Finally, elemental analyses of tube furnace residues from low- and high-density foams were similar: 73 percent C, 76 percent H, 10 percent N, and 10 percent O.

During heating to 600° C, mass balances showed that about 29 percent of the sample evolved as noncondensable (which FTIR spectra indicated were primarily CO_2 and low molecular weight organic products), about 69 percent condensables, and 2 percent remained in the furnace as condensed-phase residue. IRMP analyses showed that the condensables primarily consisted of carbonyl-, amine-, and alcohol-containing species. Periodic sampling with desorption tubes and subsequent GC-MS indicated that the primary condensable products changed with time. The time sequence in which those products evolved is as follows: (1) 3-methyl-2-butenal and cyclopentanone; (2) diaminotoluene; and (3) cyclopentanone, toluene, ethyl benzene, aminotoluene, aniline, dimethylaniline, and diaminobenzene. GPC indicated that molecular weight of condensables for both low and high density foam were also relatively low (MW <800, relative to polystyrene) with very narrow MW ranges (polydispersity <1.2). Furthermore, MS and GC-MS of the condensables indicated constituents similar to those identified in products from component-scale tests. Finally, elemental analysis was similar for furnace residue from low and high density foams: 78 percent C, 2 percent H, 11 percent N, and 9 percent O.

Decomposition Mechanisms

In general, the above results are consistent and indicate that the mechanisms and kinetics controlling decomposition of high and low density foams are similar. However, the distribution of evolved gas-phase and condensed-phase species changes with confinement. The mass transfer limitations imposed by confinement alter the relative rates of reactions controlling decomposition and can have significant impact on model development.

Decomposition of unconfined samples, for which mass transfer limitations are small, appears to occur as follows: (1) Between about 250 and 350° C, scission of the urethane linkage occurs rapidly in the polymer and produces gas-phase isocyanates and ester containing fragments that appear to have relatively low vapor pressures or to concurrently react to form more thermally stable secondary condensed-phase products. (2) Above 350 C, scission of the ester linkages occurs rapidly and produces low-molecular weight gas-phase carbonyl and hydroxy species. (3) A small fraction of the condensed-phase fragments react to form a carbonaceous residue at temperatures above 400° C. Decomposition of confined samples for which mass transfer limitations are substantial are more complicated and are still under investigation.

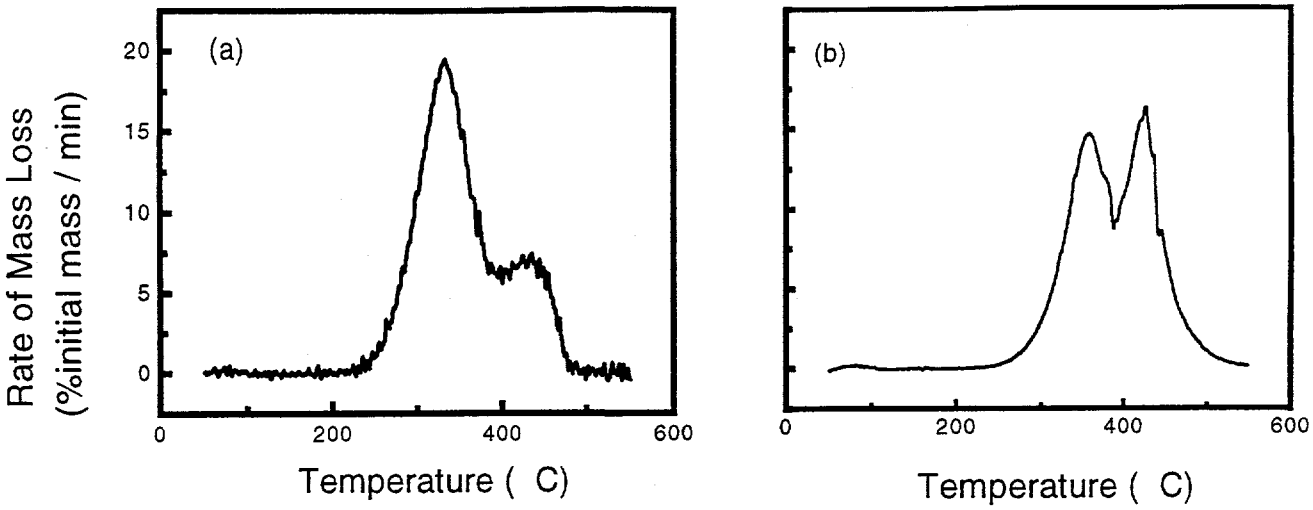

Figure 7. TGA results from 2-mg samples heated at 20° C/min: (a) unconfined, (b) partially confined, using 0.35 mm orifice.

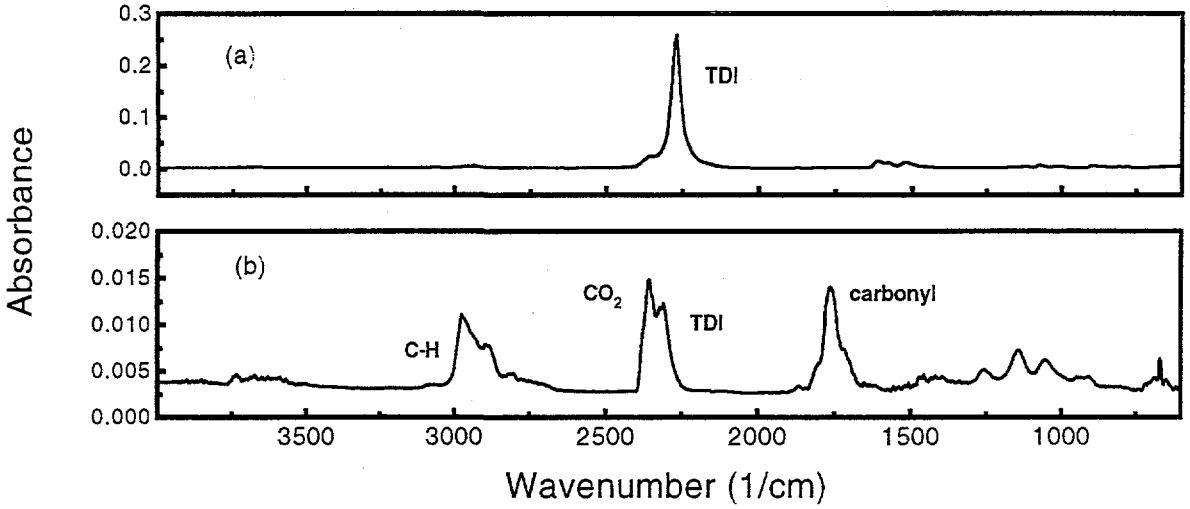

Figure 8. FTIR spectra from gases evolving during the unconfined TGA experiment illustrated in Figure 7a: (a) typical of spectra obtained at temperatures below 350° C, (b) typical of spectra obtained at temperatures above 350 °C.

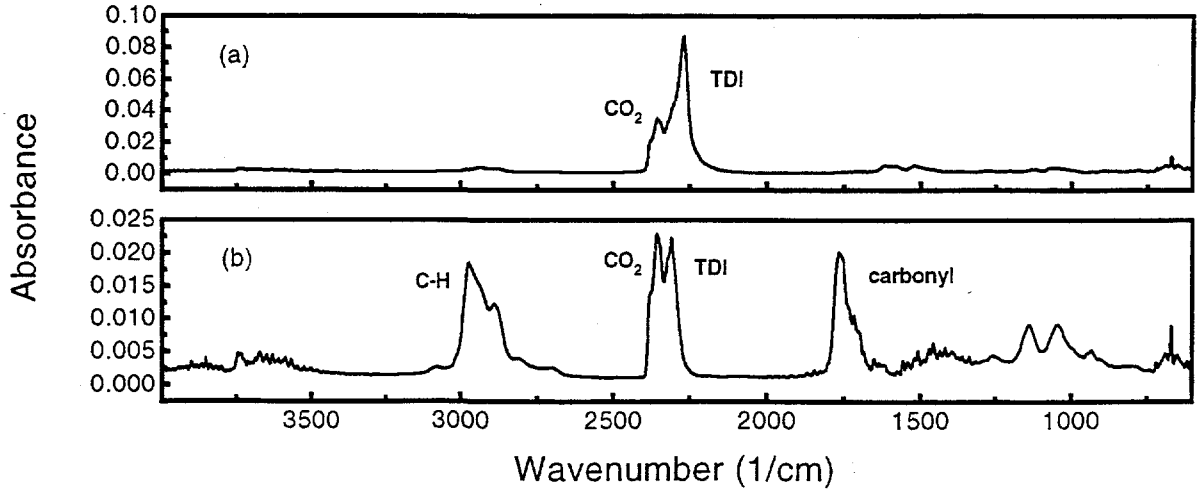

Figure 9. FTIR spectra from gases evolving during the partially confined TGA experiment illustrated in Figure 7b: (a) typical of spectra obtained at temperatures below 350° C, (b) typical of spectra obtained at temperatures above 350 °C.

4. FOAM DECOMPOSITION MODELING

Several groups studying the decomposition of large macromolecules have employed statistical network fragmentation models that form the basis of the model discussed in this paper. For example, Solomon and coworkers[2] have implemented a Monte Carlo technique to describe the breakup of coal. Fletcher et al.[3-5] have used Bethe lattice structures to obtain closed form solutions of the network statistics, as derived by Fisher and Essam.[6] These solutions parallel the determination of molecular weight distributions during polymer synthesis leading to the critical condition required to form infinite polymer networks (referred to as "gels" by Flory[7]).

Details of the PolyUrethane Foam (PUF) decomposition model will not be presented in this paper. Rather, a general description of the model and application to foam decomposition will be discussed. As shown in Fig. 10, the PUF decomposition model is based on three fundamental aspects of polymer decomposition: 1) a kinetic bond-breaking mechanism, 2) lattice statistics to describe the evolving polymer fragments, and 3) vaporization of the small polymer fragments with high vapor pressures.

The kinetic bond-breaking scheme in Fig. 10 shows the primary polymer decomposing into a secondary polymer that subsequently degrades at high temperatures. In Fig. 10, the $\mathcal{L}$, L, c_i, δ, d, and g_i, represent labile (weak) bonds in the primary polymer, labile bonds in the secondary polymer, strong or "charred" bonds, side-chains or "danglers" in the primary polymer, side-chains in the secondary polymer, and various gas species, respectively.

The activation energies for the various bond-breaking steps were obtained from the unconfined isothermal TGA experiments discussed previously and shown in Fig. 11. The single isothermal TGA samples were quickly ramped to the temperatures indicated in Fig. 11A. The dual isothermal TGA samples were ramped to 300° C and held for about two hours then ramped to the temperatures indicated in Fig. 11.B. Three of the isothermal experiments (270° C, 300° C, and 330° C) were intended to isolate the kinetics for the decomposition of the initial polymer and formation of the secondary polymer. The final three isothermal experiments were ramped to 300° C and held for approximately two hours and then ramped to the final isothermal temperatures of 380° C, 400° C, and 420° C, respectively. The intent of these final three experiments was to isolate the kinetics of the decomposition of the secondary polymer.

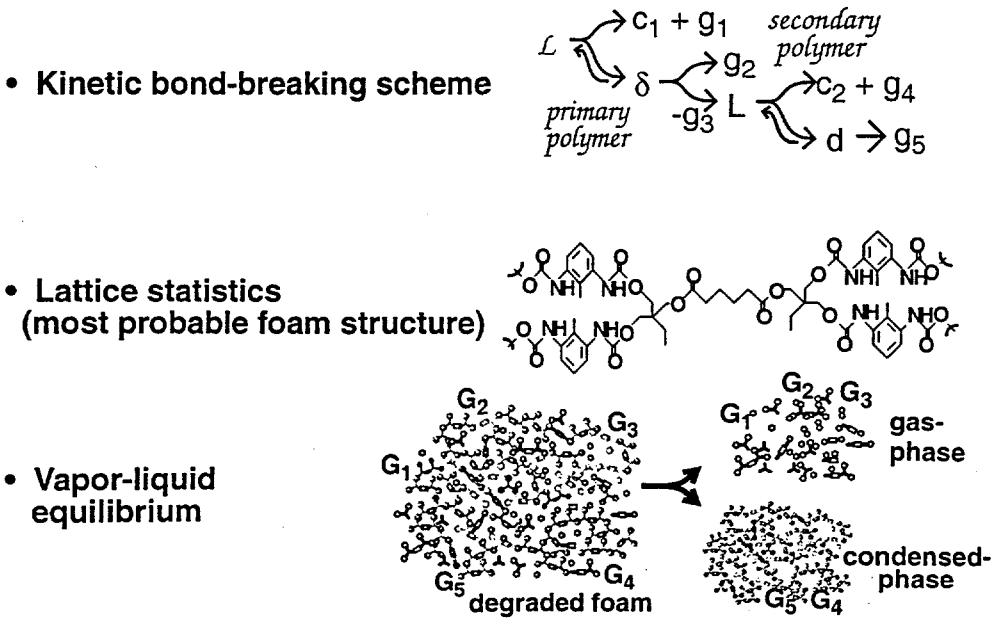

Fig. 10. Three fundamental aspects of polymer decomposition.

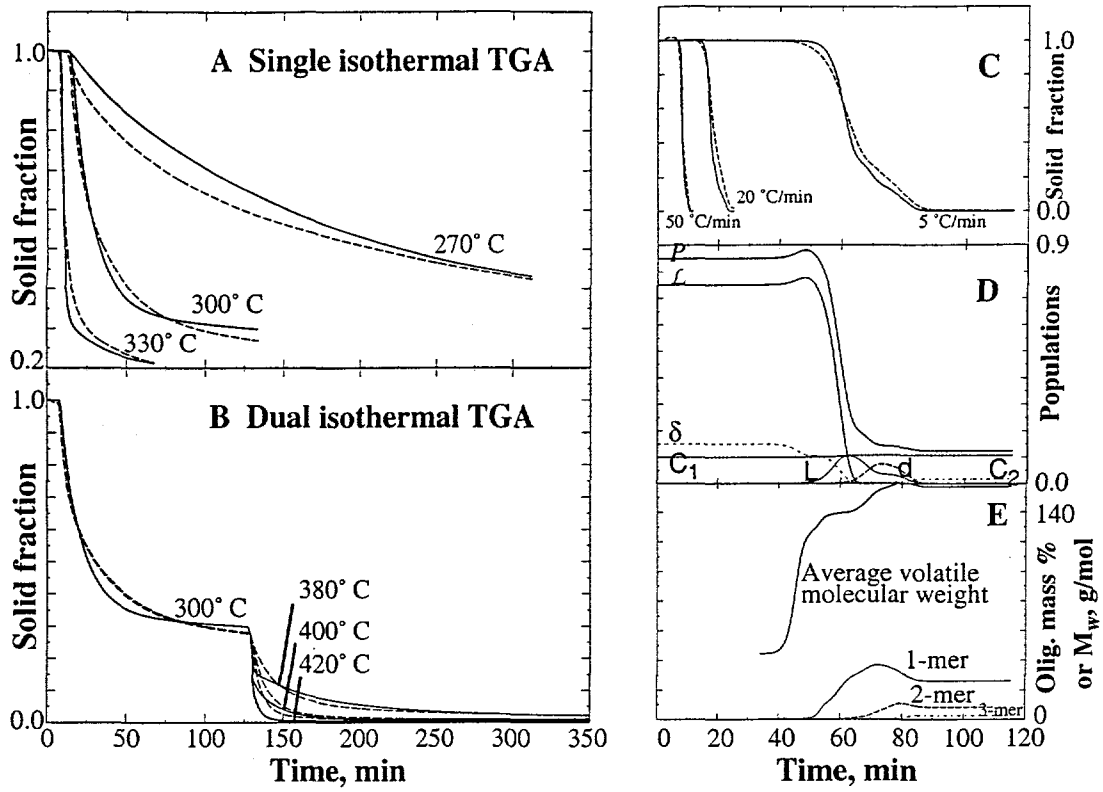

Fig. 11. Comparison of PUF predicted (solid line) and measured (dashed line) solid mass fraction for A) single isothermal TGA, B) dual isothermal TGA, and C) three nonisothermal TGA. Predicted population parameters for the 5 °C/min TGA experiment are given in D. Predicted average volatile molecular weight and various oligomer mass percents for the 5 °C/min TGA experiment are given in E.

The six isothermal TGA experiments in Figs. 11.A and 11.B were used to determine the PUF model kinetic parameters. The three nonisothermal experiments in Fig. 11.C, not used to estimate kinetic parameters, were simulated to validate the PUF model. Good agreement between predicted and measured weight loss for the three nonisothermal TGA experiments are shown in Fig. 11.C. Figures 11.D and 11.E show population parameters, the gas and oligomer mass fractions, and gas molecular weight for the 5 °C/min ramped TGA experiment. Cross-linking of two δ side-chains to form L is apparent between 40 and 60 minutes in Fig. 11.D. The reversible reaction causing reattachment of one δ side-chain to form $\mathcal{L}$ is also shown in Fig. 11.D. The increase in both $\mathcal{L}$ and L causes the bond population, p, to increase between 40 and 50 minutes. Decay of the weak bridge, $\mathcal{L}$, is shown as the side-chain population δ increases.

The most probable structure of the initial polymer, as shown in Fig. 10, was determined using synthesis information. The structures were determined by various assumptions, such as equal reactivity of the OH groups. The foam chemical structure was approximated by a Bethe lattice. The size and population of oligomers is based on the bond population, P, as determined from the kinetic bond-breaking mechanism. The fraction of the gaseous oligomers was determined in the PUF model by using a simple vapor-liquid equilibrium relationship using a combination of Dalton's law and Raoult's law. A standard multi-component isothermal flash calculation was used to determine the split between vapor and liquid.

Comparison with Component Response Experiments

The PUF decomposition model has been used successfully with a finite element heat conduction code, COYOTE,[8] using element death to simulate decomposition of rigid polyurethane foam containing an encapsulated component. This integral experiment, shown in Fig. 12, consists of a 3.8-cm diameter by 6.4-cm long right circular cylinder of 304 SS encapsulated by

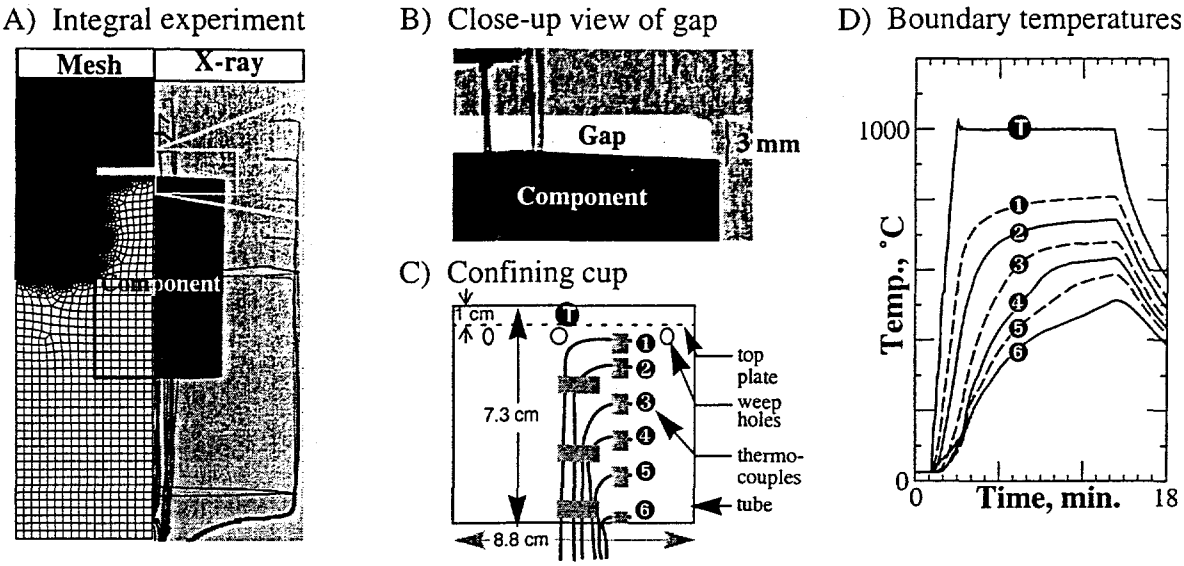

Fig. 12. A) Integral experiment showing 11,209 element mesh; B) close-up view of gap above component; C) confining cup; and D) boundary temperatures.

rigid polyurethane foam partially confined in a stainless steel can. The face of the embedded component was 3.2 cm from the heated surface. Figure 12.A also shows the mesh used in the grid-independent COYOTE simulation and an X-ray of the experimental configuration showing the 3-mm gap at the face of the cylindrical component. Resistance across the face of the component was also modeled by assuming a component surface emissivity of 0.6. The reaction enthalpy was chosen to be consistent with bond energies of polyatomic compounds. The boundary conditions for the model were set to specific temperatures along the surface of the confining cup, using data from the thermocouples, as shown in Fig. 12.C and 12.D. The temperature of the top of the cup was maintained at 1000° C, as shown in Fig. 12.D.

Figure 13 shows a comparison between X-ray images and calculated temperature profiles for the component response test at various times. The decomposition front is horizontal prior to

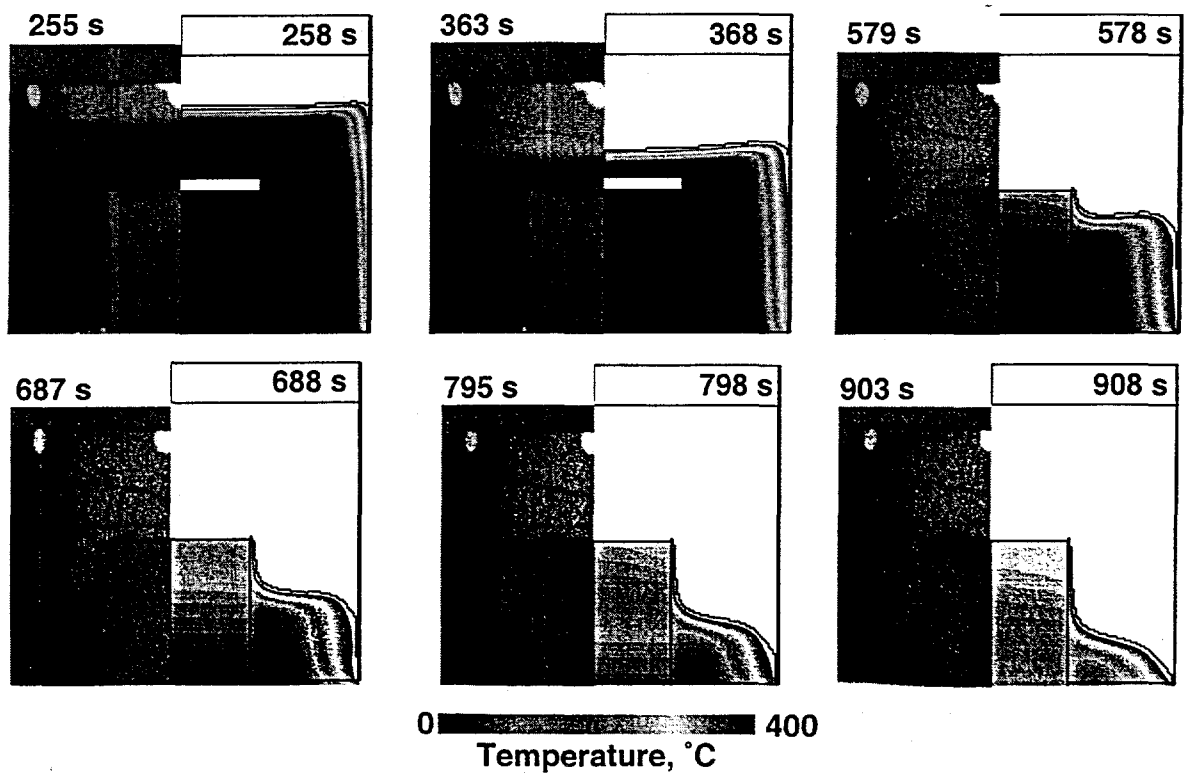

Fig. 13. X-ray images (left) and calculated temperature profiles (right).

reaching the component. As the front gets closer to the embedded component, the decomposition front curves around the component as the foam decomposes. The exact location of the decomposition front is seen as a density variation in the X-rays. COYOTE's element death option was used to remove elements when the solid fraction within individual elements was less than 0.01. The shape of the front is difficult to determine near the wall in the X-rays due to the curvature of the confinement. Nevertheless, the calculated and measured shape of the decomposition front *agree very well.*

Figure 14 shows the location of the thermocouples at the center-line and mid-radial positions. Figure 15 shows a comparison between predicted and measured center-line, mid-radial, and component temperatures, respectively. The encapsulated component appears to heat up the bulk of the foam, as shown in Fig. 15.B labeled as thermocouple ⑩. In previous experiments without an encapsulated component, all temperature measurements remained essentially constant until the decomposition front was within close proximity. With the encapsulated component, the temperatures at the various thermocouple locations are shown to increase gradually until the decomposition front is within close proximity, and the temperature increase is more rapid. This behavior is shown to be more pronounced in the experimental temperature profiles plotted in Figs. 15.B and 15.C. In Fig. 15.B, the temperature measured by thermocouple ⑩ appears to be 100 °C higher than the predicted temperature at that location. Differences between the measurement and calculation are thought to be related to premature exposure of the thermocouple to the hot radiating can and subsequent heat transfer by conduction along the thermocouple sheath to the thermocouple tip.

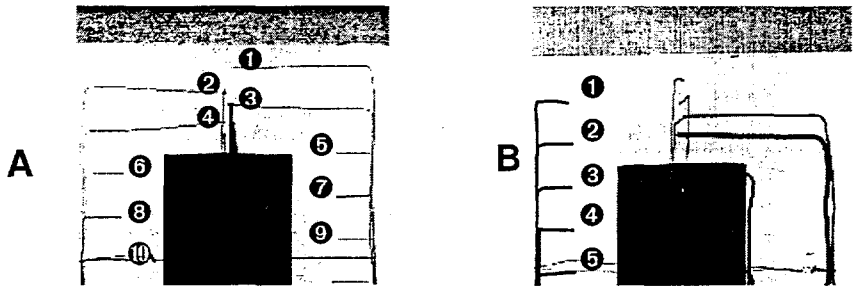

Fig. 14. A) Center-line thermocouple locations and B) mid-radial thermocouple locations.

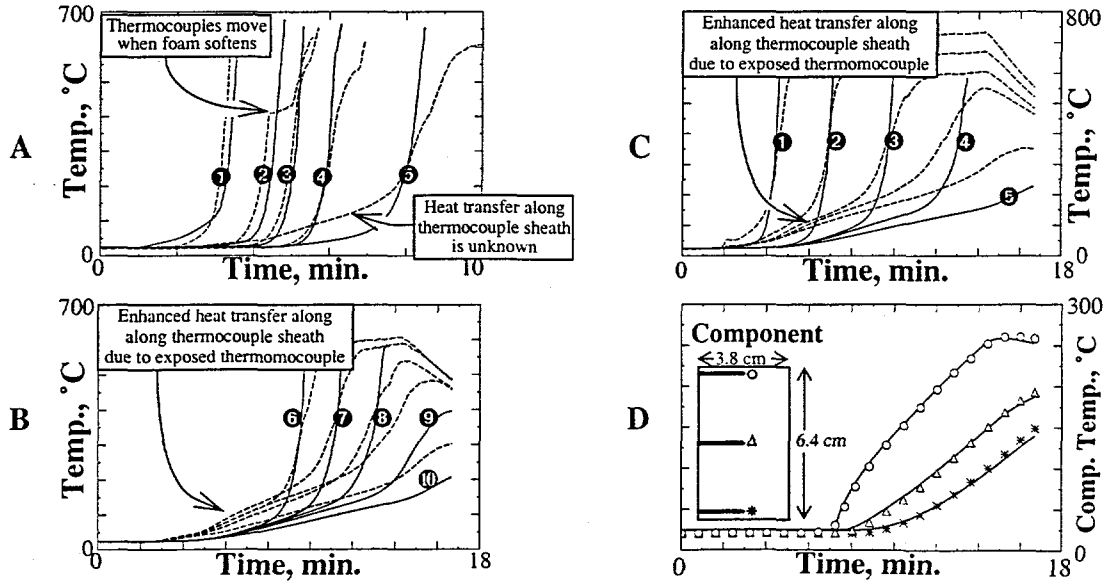

Fig. 15. Measured (dashed lines, symbols) and predicted (solid lines): A) center-line temperatures above component, B) center-line temperatures below component, C) mid-radial temperatures, and D) component temperatures.

5. SUMMARY

Ambient pressure vented one-dimensional thermal transport experiments with rigid polyurethane foam were performed under conditions consistent with fire-like thermal environments. The experiments show that thermal transport through closed cell rigid polyurethane foams has the characteristics of thermal ablation. Under a constant heat flux boundary condition, a steady state of a finite decomposition front moving with a constant recession velocity was observed. The temperature response in the foam was found to be in good agreement with the Landau[1] thermal ablation model. For confined and pressurized conditions, the progression of the decomposition front suggests a phase change phenomenon.

Decomposition of unconfined samples for which mass transfer limitations are small appears to occur as follows: (1) at temperatures between about 250° C and 350° C, scission of the urethane linkage occurs rapidly in the polymer and produces gas-phase isocyanates and ester-containing fragments, which appear to have relatively low vapor pressures or to concurrently react to form more thermally stable secondary condensed-phase products; (2) at temperatures above about 350° C, scission of the ester linkages occurs rapidly and produces low-molecular weight gas-phase carbonyl and hydroxy species; (3) a small fraction of the condensed-phase fragments react to form a carbon-aceous residue at temperatures above 400° C. In general, the mechanisms and kinetics controlling decomposition of high- and low-density foams are similar. However, the distribution of evolved gas-phase and condensed-phase species changes with confinement. The mass transfer limitations imposed by confinement alter the relative rates of reactions controlling decomposition and can have significant impact on numerical simulations. Decomposition of confined samples for which mass transfer limitations are substantially more complicated are still under investigation.

The finite element code, COYOTE, has been used with element death and the PolyUrethane Foam (PUF) decomposition model to accurately predict the decomposition of rigid polyurethane foam around an encapsulated component for configurations in which the decomposition gases can vent. Good agreement between measurements and predictions of mass loss, temperature distribution, and shape of the regression front was obtained. Small-scale experiments, consisting of three isothermal TGA experiments, three dual isothermal TGA experiments, and three nonisothermal TGA experiments, were used to develop and evaluate critical kinetic parameters of the PUF model.

6. REFERENCES

1. Landau, H.G., Quarterly of Applied Math, 8, P.31 (1950)

2. P. R. Solomon, D. G. Hamblen, R. M. Carangelo M. A. Serio, and G. V. Deshpande, G. V., Energy & Fuels, 2, 405 (1988).

3. D. M. Grant, R. J. Pugmire, T. H. Fletcher, and A. R. Kerstein, Energy & Fuels, 3, 175 (1989).

4. T. H. Fletcher, A. R. Kerstein, R. J. Pugmire, and D. M. Grant, Energy & Fuels, 4, 54 (1990).

5. T. H. Fletcher, A. R. Kerstein, R. J. Pugmire, M. S. Solum, and D. M. Grant, Energy & Fuels, 6, 414 (1992).

6. M. E. Fisher and J. W. Essam, Journal of Mathematical Physics, 2 (2), 609 (1961).

7. P. J. Flory, Principles of Polymer Chemistry, Cornell University Press., Ithaca, New York, 1953, Chapter 9.

8. D. K. Gartling, R. E. Hogan, M. W. and Glass, "COYOTE - A Finite Element Computer Program for Nonlinear Heat Conduction Problems," Version 3.0, Part 1 - Theoretical Background: SAND94-1173, Part 2 – User's Manual: SAND94-1179, Sandia National Laboratories, Albuquerque, NM, 1998.

7. Acknowledgements

The authors gratefully acknowledge the technical assistance provided by J.H. Bentz and J.G. Pantuso (integral experiments), R.S. Saunders (polymer structures and synthesis of model compounds for IR analysis), J.N. Castaneda, D.K.Derzon, J.C. Miller (all of Sandia National Laboratories), J.D. Kurtz (currently with Proctor and Gamble) and L.P. Jackson (currently at Colorado State University). Many helpful discussions regarding percolation theory with D. Grant and R. Pugmire (University of Utah) and T. H. Fletcher (Brigham Young University) are much appreciated.

This work was conducted at Sandia National Laboratories. Sandia is a multiprogram laboratory operated by Sandia Corporation, a Lockheed Martin Company, for the United States Department of Energy under Contract DE-AC04-94AL85000.